GEOPHYSICAL RESEARCH LETTERS, VOL. 36, L10304, doi:10.1029/2009GL037533, 2009

Sunda-Banda arc transition: Incipient continent-island arc collision (northwest Australia)

A. Shulgin,[1] H. Kopp,[1] C. Mueller,[2] E. Lueschen,[2] L. Planert,[1] M. Engels,[2] E. R. Flueh,[1] A. Krabbenhoeft,[1] and Y. Djajadihardja[3]

Received 29 January 2009; revised 15 April 2009; accepted 17 April 2009; published 27 May 2009.

[1] The eastern Sunda arc represents one of the few regions globally where the early stages of continent-arc collision can be studied. We studied along the western limit of the collision zone at the Sunda-Banda arc transition, where the Australian margin collides with the Banda island arc, causing widespread back arc thrusting. We present integrated results of a refraction/wide-angle reflection tomography, gravity modeling, and multichannel reflection seismic imaging using data acquired in 2006 southeast of Sumba Island. The composite structural model reveals the previously unresolved deep geometry of the collision zone. Changes in crustal structure encompass the 10–12 km thick Australian basement in the south and the 22–24 km thick Sumba ridge in the north, where backthrusting of the 130 km wide accretionary prism is documented. The structural diversity along this transect could be characteristic of young collisional systems at the transition from oceanic subduction to continent-arc collision. **Citation:** Shulgin, A., H. Kopp, C. Mueller, E. Lueschen, L. Planert, M. Engels, E. R. Flueh, A. Krabbenhoeft, and Y. Djajadihardja (2009), Sunda-Banda arc transition: Incipient continent-island arc collision (northwest Australia), *Geophys. Res. Lett.*, *36*, L10304, doi:10.1029/2009GL037533.

1. Introduction

[2] The convergence of the Indo-Australian plates and Eurasia and resulted in the formation of the Sunda and Banda island arcs. The transitional zone between the arcs is located south of Flores Island and is characterized by the change in the tectonic regime along the boundary. This segment of the plate boundary was only little investigated previously. In the scope of this study we address the problem of constraining the entire crustal scale structure and current geodynamic regime at the transitional zone using seismic reflection and wide-angle investigations and gravity modeling.

2. Tectonic Setting

[3] The plate boundary south of Sumba Island, Indonesia, is marked by a change in the tectonic regime (Figure 1) from subduction of the Indo-Australian oceanic lithosphere along the Sunda margin in the west that began ~45 m.y. ago [*Hall*, 2002] to continent - island arc collision along the Banda arc in the east [*Audley-Charles*, 1975; *Katili*, 1989; *Milsom*, 2001; *Audley-Charles*, 2004]. This margin experiences the early stages of continent-island arc collision as a result of the interaction between the Australian margin and the Banda island arc in the Pliocene [*Hall and Smyth*, 2008].

[4] Our goal is to constrain the deep crustal structure and tectonic evolution of the forearc using geophysical data collected during the RV Sonne SO-190 cruise in 2006. Our profile starts at ca. 12.5°S at the transition from the Late Jurassic oceanic lithosphere of the Argo Abyssal plain to the rifted Triassic continental crust of the Scott plateau [*van der Werff*, 1995] that is marked by the eastern termination of the Java trench at the transition to the Timor trough (Figure 1). Northwards, the oblique collision of the rifted continental crust of the Scott plateau with the forearc commenced 3–5 Ma ago [*Harris*, 1991] at a rate of ~7 cm/yr [*Curray*, 1989]. The current convergence rate at the Timor trough is ~15 mm/yr [*Bock et al.*, 2003] and it is manifested in back arc thrusting [*Silver and Reed*, 1988]. The Sumba Block, farther north, is believed to be an isolated tectonic block trapped between the trench and the volcanic arc (see *Rutherford et al.* [2001] and *Hall and Smyth* [2008] for discussion). Ridge structures of the Sumba Ridge include the submarine basement high, extending from Sumba Island to Savu Island and then merging with outer high crest towards Timor Island (Figure 1) [*Silver et al.*, 1983]. The basement of the ridge is dated from >80 to ~18 Ma, as inferred from the outcrops of intrusives and volcanic rocks together with sediments on Sumba and Savu Islands [*Karig et al.*, 1987], which might have been a part of the Paleogene Sumba-Banda forearc [*Hall and Smyth*, 2008].

[5] The origin of the abnormal width of the forearc south of Flores Island is enigmatic (Figure 1). Seismicity deeper than 30 km is absent between the islands of Sumba and Timor, while further north common earthquakes deeper than 100 km [*Engdahl and Villaseñor*, 2002] suggest the presence of the subducting slab below the Banda island arc, further confirmed by geochemical data from Flores Island [*Elburg et al.*, 2004]. However, most volcanic rocks of the Banda islands consist of primitive basalts typical of a volcanic arc built on oceanic lithosphere [*Hamilton*, 1988]. The complex basement thus reflects different periods of extension, subduction, and collision in Eastern Indonesia [*Hall and Smyth*, 2008].

3. Data Acquisition and Modeling

[6] Here we present a Vp seismic tomography model along the Sunda - Banda arc transition, further constrained by gravity modeling. Marine seismic investigations (Figure 1) were carried out by multichannel seismic reflection profiling (MCS), accompanied by gravity measurements, and seismic refraction profiling with ocean-bottom seismometers (OBS)

[1]Leibniz Institute of Marine Sciences, IFM-GEOMAR, Kiel, Germany.
[2]Federal Institute for Geosciences and Natural Resources, Hannover, Germany.
[3]Agency for the Assessment and Application of Technology, Jakarta, Indonesia.

0094-8276/09/2009GL037533$05.00

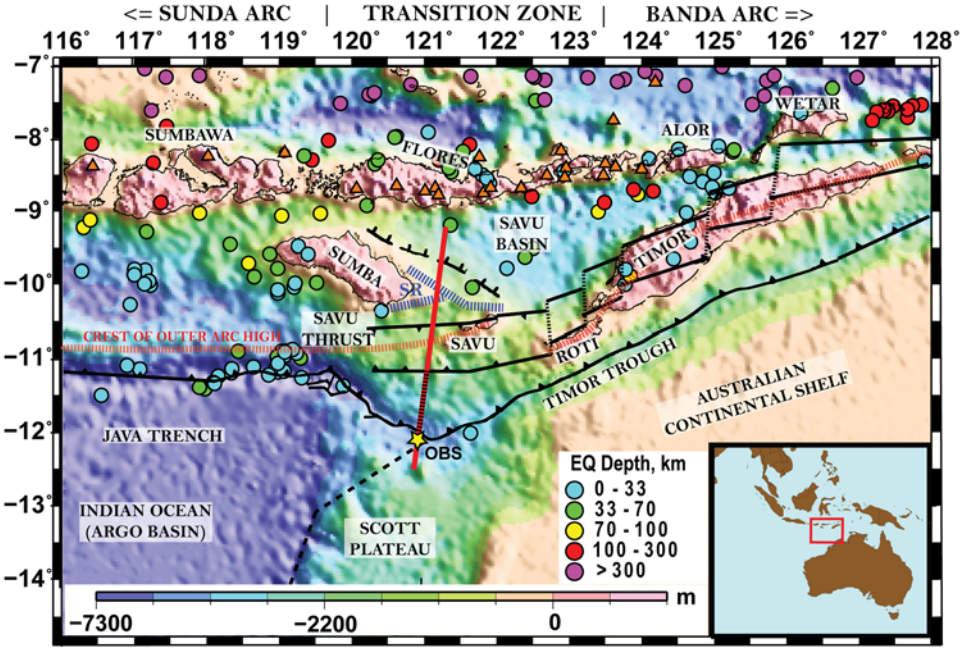

Figure 1. Simplified tectonic and bathymetric map of the Sunda-Banda Arc transition. Red line - seismic profile discussed in this study. Dashed red-black line - the MCS section shown in Figure 2. Yellow star - OBS location shown in Figure 2. Red triangles - active and Neogene volcanoes. Dashed blue line - a submarine Sumba Ridge (SR). Dashed red line - the crest of the outer forearc high. Black lines - faults [after *Rutherford et al.*, 2001; *Audley-Charles*, 2004]. Relocated earthquakes in the region are shown by filled circles, color-coded with depth [after *Engdahl and Villaseñor*, 2002].

and hydrophones (OBH) [*Mueller et al.*, 2008] (Text S1 of the auxiliary material).[1]

[7] The seismic velocity model was constrained by joint refraction/reflection 2D tomographic inversion [*Korenaga et al.*, 2000]. Data from a total of 36 stations were used as input to the tomographic modeling. First, ~16,000 first arrival phases with offsets of up to 120 km were picked; subsequently, ~4,000 reflected phases were added to the dataset. We applied a "top to bottom" approach with a simple layered starting model, initially constraining the model only for the near offsets and then increasing the depth extent of the ray coverage to constrain the entire model space. The structure of the sediments and the upper crust was controlled by the MCS data (Figure 2), thus constraining the upper section of the profile in great detail. Calculated uncertainty of traveltimes for ~85% of the all picked phases lies within the picking error range of 50 ms.

[8] The resulting Vp seismic tomography model was extended 100 km to the north and south and to a depth of 75 km to be used in forward gravity modeling. Velocities were converted to densities [*Christensen and Mooney*, 1995; *Carlson and Herrick*, 1990] and the subducting slab extended to 75 km depth underneath the island arc, where the deep seismicity commences. A constant density of 3.35 g/cm^3 was assumed for the mantle (Figure 3c).

4. Results (South to North Along 121°E)

4.1. Scott Plateau: Australian Crust

[9] The 2 km thick sedimentary cover of the Java trench has average Vp seismic velocities of 2–3 km/s in the trench section. A facies transition from deep marine fine grained carbonates to Upper Cretaceous shallow marine clastic deposits [*Stagg and Exon*, 1979] recognized in the MCS data forms the décollement at ~5 km depth (Figure 2a). A mud diapir observed at CDP 12900 (Figure 2) may be related to high pore pressures in the lower unit, also a series of linear mud diapirs nearby have been reported by *Breen et al.* [1986]. At depths between 6 km and 10 km Vp below the reflection gradually change from 3.5 km/s to 5 km/s (Figure 3a). Upper crustal velocities are ~6.0 km/s and increase to 6.7–7.0 km/s in the lower crust (Figure 3a), as revealed by the Puc and Plc phases (Figure 2c). The transition from the upper to the lower crust is marked by a strong reflection well documented by Pic phases. The Moho is recovered by the PmP phases at a depth of 20 km and is apparently dipping northwards at an angle of ~1°. Thus, the thickness of the crystalline crust reaches 10 to 12 km only. Although a continental crust with an Australian affinity was proposed to exist further east [*Kaneko et al.*, 2007], these values are in contrast to the typical thickness of the continental crust in NW Australia [*Collins et al.*, 2003] and at other continental shelves [e.g., *Ritzmann and Faleide*, 2007].

4.2. Frontal Prism and the Neogene Accretionary Wedge

[10] Imbricate thrusting (Figure 2a) and relatively low seismic velocities of 2.5–3.5 km/s down to 6–7 km depth indicate the presence of a large, ~20 km wide, frontal prism arcward of the deformation front (51 km distance). The ~60 km wide Neogene accretionary prism, imaged in the MCS data and confirmed by Vp values <4.0 km/s, is located between 85–130 km profile distance and forms the middle prism, app. bounded by the 3 km/s isoline. It is characterized by a laterally inhomogeneous velocity field and thrust fault-

[1] Auxiliary materials are available in the HTML. doi:10.1029/2009GL037533.

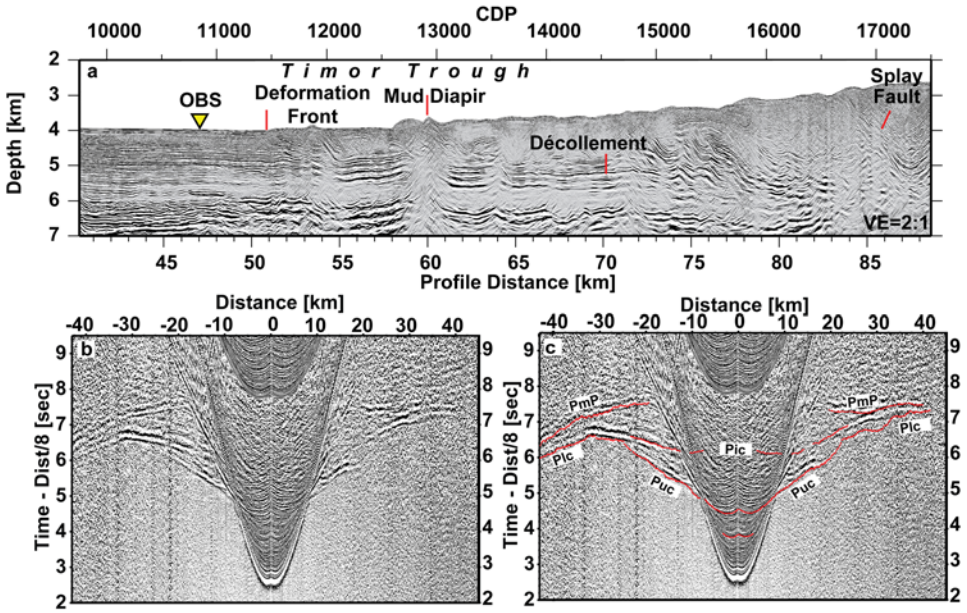

Figure 2. (a) MCS depth migrated section for the areas around Timor Trough (location shown in Figure 1). (b and c) example of the OBS data used in this study. Yellow triangle - the OBS position, shown in Figure 2b and 2c. Red dots show the computed travel-times of the seismic rays shot through the tomography model.

ing, observed in the MCS data. A system of splay faults that originate at the décollement and trend upwards at the angle of ~20° marks the transition to the middle prism (Figure 2a). The trench fill is composed of Mesozoic and Cenozoic sediments, eroded from the Australian continental shelf, with the lower part composed of clastic and volcano-clastic rocks, and the upper part composed of deep-water carbonates [*Breen et al.*, 1986]. The upper half of the sediments in the Timor trough is incorporated into the frontal prism. The lower 1000–1200 m of the clastic unit are currently bypassing the frontal prism (Figures 2a and 3a) and most likely underplate below the accretionary prism. The décollement is traced as a high-amplitude reflector for 30 km landward of the deformation front and extends to a depth of 6 km.

4.3. Paleo-accretionary Wedge

[11] The central section of the profile (140–210 km) suffers from limited energy penetration due to anomalous high attenuation and/or significant scattering. The opaque seismic character of the forearc high as observed both in the wide-angle and MCS data together with moderate Vp in the sedimentary cover (ranging from 2 km/s below the sea floor to 5 km/s at a depth of 10 km) (Figure 3a) suggests that the forearc high is composed of pre-Neogene accreted material that forms the paleo-accretionary complex. This material is probably derived from the stratigraphic units currently present on the Scott Plateau, which are composed of Jurassic sandstones overlain by Cretaceous marine shales [*Breen et al.*, 1986] and could have accumulated during the initial subduction of the passive Australian margin [*van der Werff et al.*, 1994] or during the subduction of Jurassic oceanic lithosphere of the Banda embayment (as shown by *Hall and Smyth* [2008]). Geologically the prism may be linked to the southern part of Timor, underlain by the outcropping Kolbano Complex, including Jurassic-Pliocene folded sediments of Australian origin, representing a segment of the accretionary complex [*Karig et al.*, 1987]. As suggested by numerical modeling of collisional margin settings [*Selzer et al.*, 2008], the opaque seismic character of the deeper portion may be caused by basally stacked packages of highly scattering rock fabric thus inhibiting deep energy penetration.

4.4. Sumba Ridge

[12] The crest of the Sumba ridge [*Silver et al.*, 1983] is located at 250 km profile distance; the basement top (app. corresponding to the 4 km/s isoline) is at a depth of 3 km below sea level at the crest and slopes down to 9 km depth in the south and to 6 km depth in the north (Figure 3a). A sharp velocity change in the upper crust at ~200 km distance marks the southern limit of the Sumba ridge. A vertical displacement of the basement occurs at 260 km underneath a small sedimentary basin and again at the northern edge of the ridge (at 310 km). The ridge is covered by sediments (presumably eroded from the Sumba, Savu and Timor islands) with a thickness of 0.5 km increasing to more than 2 km in thickness at its flanks. A crustal reflection observed below the entire northern portion of the profile at depths of 15–17 km probably corresponds to the transition between the upper and the lower crust (Figure 3a). Vp velocities vary from 5.5 km/s to 6.4–6.5 km/s in the upper crust, and from 6.7–6.8 km/s to 7.1 km/s in the lower crust and are typical of a mature arc massif or possibly of a fragment of a continental crust, which can be linked to the existence of a volcanic arc in the eastern Indonesia during the Paleogene, traces of which may be found in the highest nappes of Timor and other Banda islands [*Hall and Smyth*, 2008]. The PmP phases indicate the slightly southwards dipping Moho at a depth of ~26 km below the Sumba ridge. Available Pn phases indicate Vp ~ 8.0 km/s in the forearc mantle.

4.5. Savu Basin

[13] The transition from the Sumba ridge to the Savu basin (at 310 km) is marked by sea floor deepening and an increase in sedimentary thickness. The sedimentary fill eroded from

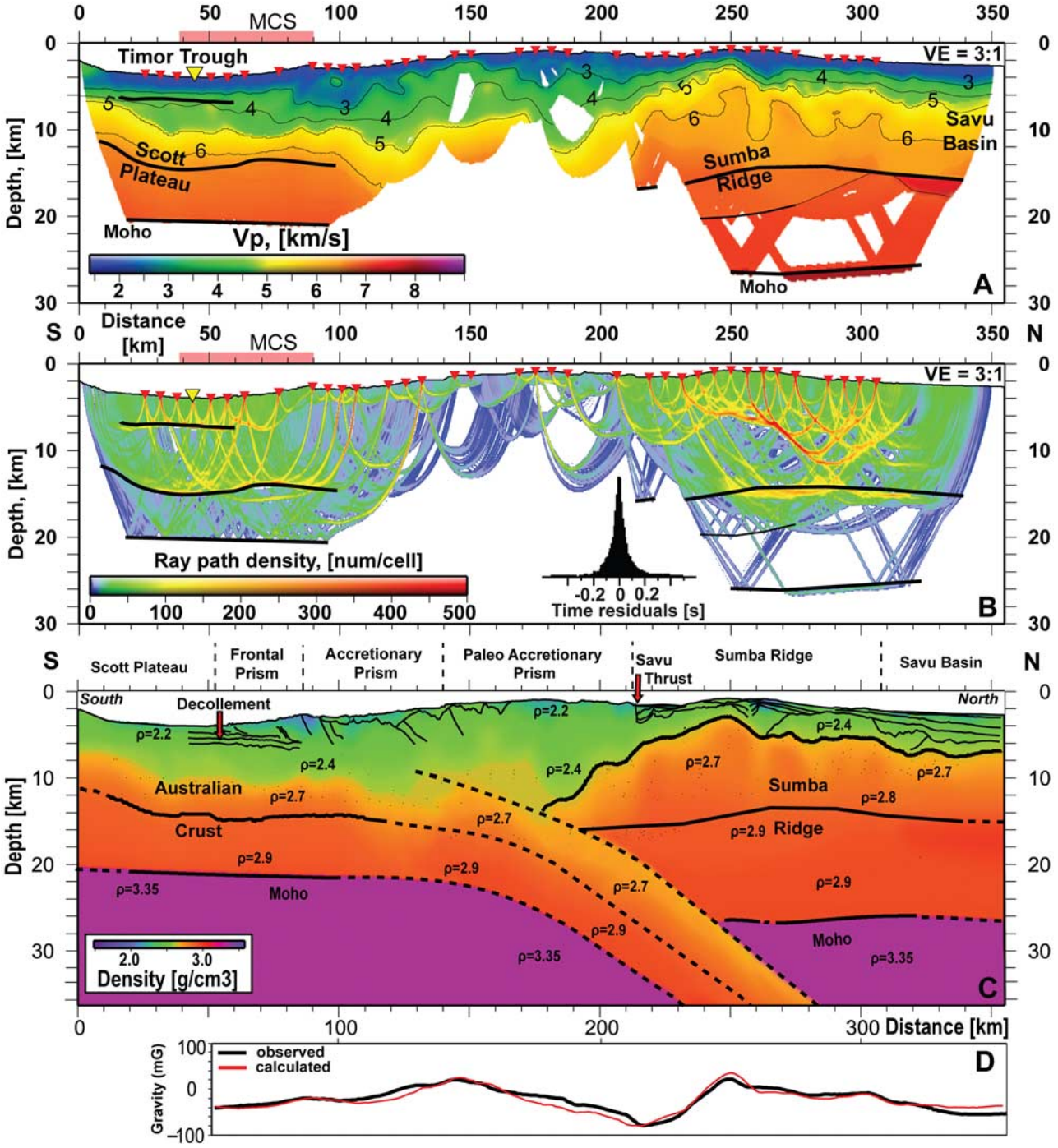

Figure 3. (a) Results of seismic tomography and gravity modeling a) Recovered tomography model, black lines - seismic reflectors. Red triangles - the OBS/OBH locations. Yellow triangle - OBS location (Figure 2). Pink line along the distance axis - MCS data shown in Figure 2. (b) Ray path coverage obtained during the tomographic inversion. Insert shows the time residuals distribution. (c) Combined model. Background color and numbers - density based the tomography and gravity results. Thin solid black lines - reflection horizons from the MCS data. Thick black lines - interfaces used in the gravity modeling. Interfaces not seismically resolved - dashed lines. (d) results of gravity modeling. Red line - observed data; black line - calculated gravity field.

the island arc [*Audley-Charles*, 2004] reaches a total thickness of 3 km with Vp velocities ranging from <2 km/s to 4 km/s (Figure 3a). The basement topography and sedimentary layering are consistent with earlier seismic reflection profiles in the Savu basin [*Karig et al.*, 1987; *Breen et al.*, 1986; *van der Werff et al.*, 1994]. Our wide-angle data for the first time document the Moho at a depth of 26 km.

4.6. Crustal Structure From Seismic Inversion and Gravity Modeling

[14] Figure 3c shows the tectonic model based on the results of the reflection seismic imaging, the wide-angle tomography, and gravity modeling. In the south, the crust of Australian affinity is dipping arcward at an angle of ~10–11°. The 10–12 km thick crystalline crust of the Scott plateau as a promontory of the Australian continent (described above) underthrusts the Banda forearcs.

[15] Between the Sumba ridge and the trough, the accretionary complex shows thrusting and represents a nascent orogeny, forced by post-Pliocene convergence and buoyant uplift associated with the transition from active oceanic subduction to continent-island arc collision. The complex is composed of a frontal prism, where active frontal accretion is documented, juxtaposed against a 130 km wide accretionary prism. The central section of the profile (140–210 km distance) consists of the paleo-accretionary prism bounded northwards by the Sumba ridge, which acted as backstop to the paleo-prism during the time of accretion. Most likely the paleo-prism was added to the Sumba ridge, during the SSW tectonic escape of Sumba Island, caused by the initial contact of Australia and the Banda arc [*Rutherford et al.*, 2001]. The Savu thrust marks the tectonic transition from the accretionary wedge to the tectonic units of the Sumba ridge. Vertical growth of the prism facilitated backthrusting over the Sumba ridge along the Savu thrust [*Silver and Reed*, 1988], however, motion along the Savu thrust must primarily be driven by high basal friction due to the low relief difference between the prism and the ridge. The crustal thickness of the Sumba ridge is ~23 km with crustal densities ranging from 2.65 g/cm^3 to 2.90 g/cm^3. Towards the island arc, the thickness of the crystalline crust is ~20 km below the Savu basin with the upper plate Moho at a depth of ~26–27 km, as also supported by gravity modeling. The crustal thickness is increased compared to the Lombok basin west of Sumba Island, which is underlain by 7 km thick crust (E. Lueschen et al., Structure, evolution and tectonic activity at the Eastern Sunda forearc, Indonesia, from marine seismic investigations, submitted to *Tectonophysics*, 2009).

5. Discussion

[16] Newly acquired seismic reflection/refraction and gravity data east and south of Sumba Island resolve the deep crustal structure at the Sunda-Banda arc transition (Figure 3c). The current system can be regarded as a precursor of a fold-and-thrust belt, which may develop in the forearc as the collision progresses. The wide-angle seismic data resolve the full crustal structure of the Sumba ridge and the Savu basin and for the first time provide the geophysical background for geodynamic models of nascent collisional systems. The observed variations in crustal structure along the profile may be typical for tectonic settings with continental margins approaching island arcs. The observed variations in the crustal structure along the profile are similar to the present structure around Taiwan, formed by the transition from subduction to collision of Eurasia and the Philippine Sea plate [*Huang et al.*, 2006; *Sibuet and Hsu*, 2004].

[17] **Acknowledgments.** We would like to thank Captain Meyer and the crew of R/V Sonne and the SINDBAD Working group for their enormous help in collecting and processing of the data. Authors express great gratitude to Jun Korenaga for the discussion on seismic tomography and Tomo2D code. We would like to thank the GRL editor Fabio Florindo and reviewers for their help in improving the manuscript. The SINDBAD project is funded by the German Federal Ministry of Education and Research (BMBF) (grants 03G0190A and 03G0190B).

References

Audley-Charles, M. G. (1975), The Sumba fracture: A major discontinuity between eastern and western Indonesia, *Tectonophysics*, *26*, 213–228.

Audley-Charles, M. G. (2004), Ocean trench blocked and obliterated by Banda forearc collision with Australian proximal continental slope, *Tectonophysics*, *389*, 65–79.

Breen, N. A., E. A. Silver, and D. M. Hussong (1986), Structural styles of an accretionary wedge south of the island of Sumba, Indonesia, revealed by SeaMARC II side scan sonar, *Geol. Soc. Am. Bull.*, *97*, 1250–1261.

Bock, Y., L. Prawirodirdjo, J. F. Genrich, C. W. Stevens, R. McCaffrey, C. Subarya, S. S. O. Puntodewo, and E. Calais (2003), Crustal motion in Indonesia from Global Positioning System measurements, *J. Geophys. Res.*, *108*(B8), 2367, doi:10.1029/2001JB000324.

Carlson, R. L., and C. N. Herrick (1990), Densities and porosities in the oceanic crust and their variations with depth and age, *J. Geophys. Res.*, *95*, 9153–9170.

Christensen, N. I., and W. D. Mooney (1995), Seismic velocity structure and composition of the continental crust: A global view, *J. Geophys. Res.*, *100*, 9761–9788.

Collins, C. D. N., B. J. Drummond, and M. G. Nicoll (2003), Crustal thickness patterns in the Australian continent, *Geol. Soc. Am. Spec. Pap.*, *372*, 121–128.

Curray, J. R. (1989), The Sunda arc: A model for oblique plate convergence, *Neth. J. Sea Res.*, *24*, 131–140.

Elburg, M. A., M. J. van Bergen, and J. D. Foden (2004), Subducted upper and lower continental crust contributes to magmatism in the collision sector of the Sunda-Banda arc, Indonesia, *Geology*, *32*, 41–44.

Engdahl, E. R., and A. Villaseñor (2002), Global seismicity: 1900–1999, in *International Handbook of Earthquake and Engineering Seismology*, pp. 665–690, Academic, San Diego, Calif.

Hall, R. (2002), Cenozoic geological and plate tectonic evolution of SE Asia and the SW Pacific: Computer-based reconstructions, model and animations, *J. Asian Earth Sci.*, *20*, 353–434.

Hall, R., and H. R. Smyth (2008), Cenozoic arc processes in Indonesia: Identification of the key influences on the stratigraphic record in active volcanic arcs, *Geol. Soc. Am. Spec. Pap.*, *436*, 27–54.

Hamilton, W. B. (1988), Plate tectonics and island arcs, *Geol. Soc. Am. Bull.*, *100*, 1503–1527.

Harris, R. A. (1991), Temporal distribution of strain in the active Banda orogen: A reconciliation of rival hypotheses, *J. Southeast Asian Earth Sci.*, *6*, 373–386.

Huang, C.-Y., P. B. Yuan, and S.-J. Tsao (2006), Temporal and spatial records of active arc-continent collision in Taiwan: A syntasis, *Geol. Soc. Am. Bull.*, *118*, 274–288.

Kaneko, Y., S. Maruyama, A. Kadarusman, T. Ota, M. Ishikawa, T. Tsujimori, A. Ishikawa, and K. Okamoto (2007), On-going orogeny in the outer-arc of the Timor-Tanimbar region, eastern Indonesia, *Gondwana Res.*, *11*, 218–233.

Karig, D., A. Barder, T. Charlton, S. Klemperer, and D. Hussong (1987), Nature and distribution of deformation across the Banda Arc: Australia collision zone at Timor, *Geol. Soc. Am. Bull.*, *98*, 18–32.

Katili, J. A. (1989), Review of past and present geotectonic concepts of eastern Indonesia, *Neth. J. Sea Res.*, *24*, 103–129.

Korenaga, J., et al. (2000), Crustal structure of the southeast Greenland margin from joint refraction and reflection seismic tomography, *J. Geophys. Res.*, *105*, 21,591–21,614.

Milsom, J. (2001), Subduction in eastern Indonesia: How many slabs?, *Tectonophysics*, *338*, 167–178.

Mueller, C., et al. (2008), From subduction to collision: The Sumba-Banda Arc transition, *Eos Trans. AGU*, *89*, 49–50.

Ritzmann, O., and J. I. Faleide (2007), Caledonian basement of the western Barents Sea, *Tectonics*, *26*, TC5014, doi:10.1029/2006TC002059.

Rutherford, E., K. Burke, and J. Lytwyn (2001), Tectonic history of Sumba Island, Indonesia, since the Late Cretaceous and its rapid escape into forearc in the Miocene, *J. Asian Earth Sci.*, *19*, 453–479.

Selzer, C., S. J. H. Buiter, and O. A. Pfiffner (2008), Numerical modeling of frontal and basal accretion at collisional margins, *Tectonics*, *27*, TC3001, doi:10.1029/2007TC002169.

Sibuet, J.-C., and S.-K. Hsu (2004), How was Taiwan created?, *Tectonophysics*, *379*, 159–181.

Silver, E. A., and D. L. Reed (1988), Backthrusting in accretionary wedges, *J. Geophys. Res.*, *93*, 3116–3126.

Silver, E. A., D. L. Reed, and R. McCaffrey (1983), Back arc thrusting in the eastern Sunda arc, Indonesia: A consequence of arc-continent collision, *J. Geophys. Res.*, *88*, 7429–7448.

Stagg, H. M. J., and N. F. Exon (1979), Western margin of Australia: Evolution of a rifted arch system—Discussion, *Geol. Soc. Am. Bull.*, *90*, 795–797.

van der Werff, W. (1995), The evolution of the Savu Forearc Basin, Indonesia (Forearc response to arc/continent collision), *J. Mar. Petrol. Geol.*, *12*, 247–262.

van der Werff, W., D. Kusnida, and H. Prasetyo (1994), On the origin of the Sumba forearc basement, *J. Mar. Petrol. Geol.*, *11*, 363–374.

Y. Djajadihardja, Agency for the Assessment and Application of Technology, Jl.M.H. Thamrin No. 8, Jakarta 10340, Indonesia.

M. Engels, E. Lueschen, and C. Mueller, Federal Institute for Geosciences and Natural Resources, Stilleweg 2, D-30655 Hannover, Germany.

E. R. Flueh, H. Kopp, A. Krabbenhoeft, L. Planert, and A. Shulgin, Leibniz Institute of Marine Sciences, IFM-GEOMAR, Wischhofstr. 1-3, D-24148 Kiel, Germany. (ashulgin@ifm-geomar.de)